

---

## **Fi<sub>x</sub> CONTROLLER: AN INSTRUMENT TO AUTOMATICALLY ADJUST INSPIRED OXYGEN FRACTION USING FEEDBACK CONTROL FROM A PULSE OXIMETER**

*Daniel B. Raemer, PhD,<sup>1,3</sup> Xin-Bao Ji, PhD,<sup>2</sup> and George P. Topulos, MD<sup>2,3</sup>*

---

---

Raemer DB, Xin-Bao Ji, Topulos GP. Fi<sub>x</sub> Controller: An instrument to automatically adjust inspired oxygen fraction using feedback control from a pulse oximeter.

J Clin Monit 1997; 13: 91–101

**ABSTRACT. Objective.** To develop an instrument to help prevent pulmonary O<sub>2</sub> toxicity, a syndrome that manifests itself in adult intensive care patients. **Methods.** We designed, built, and tested a device that controls FiO<sub>2</sub> exposure using oxygen saturation measured with a pulse oximeter (SpO<sub>2</sub>) in a negative feedback control system. A target SpO<sub>2</sub> is designated by the clinician and the system adjusts the FiO<sub>2</sub> from a mechanical ventilator so as to minimize the difference between the measured SpO<sub>2</sub> and the target. Important elements of the system include a conservative artifact rejection algorithm, a gain-scheduled sampled-data proportional-integral-derivative (PID) controller, and a safety system to prevent inspired mixtures with undesirably low FiO<sub>2</sub> due to device failure. **Results.** The control system was tuned in a series of animal experiments. Acceptable clinical response of the system was obtained using a gain-scheduled controller algorithm whereby the gain of the proportional term of a PID controller was adjusted based on the error signal and measured minute ventilation. Also, the artifact rejection algorithm and safety systems were successfully tested using simulation. **Conclusions.** Testing the effectiveness of this instrument will require comparison with manual control of FiO<sub>2</sub> in an appropriately designed trial.

**KEY WORDS.** Monitoring: oxygen saturation. Equipment: ventilators, pulse oximetry, oxygen analyzers. Oxygen: toxicity.

---

Pulmonary O<sub>2</sub> toxicity is a complex syndrome that is seen in adult intensive care patients [1]. It is generally associated with other respiratory system problems that require the prolonged use of high FiO<sub>2</sub> to prevent arterial hypoxemia. The manifestations of pulmonary oxygen toxicity may include tracheobronchitis, mechanical dysfunction, gas exchange abnormalities, and morphologic changes.

Therapy for pulmonary oxygen toxicity is supportive, the most important measure being prevention by administering the lowest FiO<sub>2</sub> that results in an acceptable PaO<sub>2</sub>. There is no evidence concerning the threshold or time-concentration relationship involved in the development of a chronic pulmonary lesion, but, FiO<sub>2</sub> below 0.5 – 0.6 is generally considered safe for extended periods of time [2].

Yu et al designed a system to control the FiO<sub>2</sub> exposure using oxygen saturation measured with a pulse oximeter in a negative feedback control system [3]. They used a proportional-plus-integral controller and an improved multiple-model adaptive control algorithm to provide relatively constant dynamic performance of the system with rapid changes in the patient, ventilator, or

From the <sup>1</sup>Department of Anesthesia, Massachusetts General Hospital, <sup>2</sup>Department of Anesthesia, Brigham and Women's Hospital and <sup>3</sup>Department of Anaesthesia, Harvard Medical School.

Received May 23, 1996. Accepted for publication Jul 22, 1996.

Address correspondence to Daniel B. Raemer, PhD, Department of Anesthesia, Massachusetts General Hospital, Boston, MA 02114, USA.

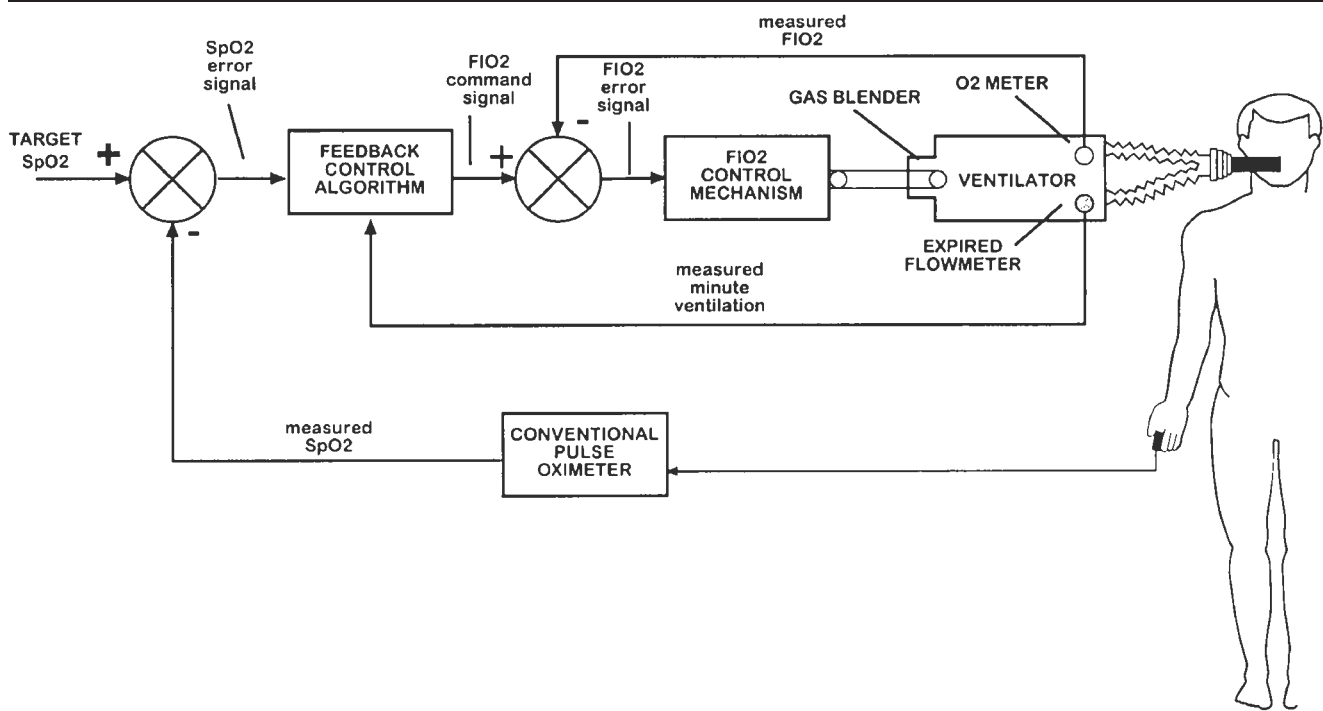


Fig. 1. Block diagram of  $F_{I_x}$  feedback control system. A target  $SpO_2$ , as set by the clinician, is compared to the measured  $SpO_2$  by a conventional pulse oximeter. The difference comprises an  $SpO_2$  error signal that is processed by a feedback control algorithm. The resulting  $F_{IO_2}$  command signal specifies a particular value. This value is compared to the measured  $F_{IO_2}$  as determined by an  $O_2$  sensor in the inspired limb of a ventilator breathing circuit. The  $F_{IO_2}$  error signal is processed by the  $F_{IO_2}$  control mechanism, which rotates the  $F_{IO_2}$  control knob of a ventilator gas blender. The response of a ventilated subject is, in turn, fed back as a new measured  $SpO_2$  via the pulse oximeter. The system works to minimize the  $SpO_2$  error signal, thereby driving the patient's  $SpO_2$  to the value of the target  $SpO_2$ .

sensor gain. Tehrani also proposed a similar system that used a proportional-plus-integral controller with a set-point adaptation supervisor to avoid periods of high  $F_{IO_2}$  [4]. Neither of these authors addressed the problems of artifactual  $SpO_2$  signals which are very common nor adequately addressed the therapeutic objectives of prevention of both hypoxemia and oxygen toxicity. We developed a system similar in design to that of Yu using gain-scheduled sampled-data control and an algorithm to provide clinically acceptable performance in the face of artifactual  $SpO_2$  signals. In addition, this system determines the  $F_{IO_2}$  necessary to achieve a desired  $SpO_2$  (defined as the  $F_{I_x}$ , where  $F_I$  stands for inspired fraction and  $x$  represents the desired  $SpO_2$ , generally in the range 90%–99%) as an indicator of the severity of respiratory disease [5].

## SYSTEM DESIGN

As depicted in Figure 1, a target  $SpO_2$  (e.g. 95%) is designated by the clinician. The target  $SpO_2$  is compared with the  $SpO_2$  measured with a conventional pulse oximeter.

The difference comprises an error signal ( $SpO_2$  error signal) that is processed by a feedback control algorithm. The feedback controller computes a value ( $F_{IO_2}$  command signal) as an output. The  $F_{IO_2}$  command signal is compared with the measured  $F_{IO_2}$  as determined by an oxygen sensor in the inspired limb of a ventilator. The difference comprises an error signal ( $F_{IO_2}$  error signal) that is processed by the  $F_{IO_2}$  control mechanism. As directed by the  $F_{IO_2}$  control mechanism, a motor rotates the  $F_{IO_2}$  control knob of a ventilator gas blender. The resulting patient response is, in turn, fed back as a new value of  $SpO_2$  as determined by the pulse oximeter. The system works to minimize the  $SpO_2$  error signal, thereby driving the measured  $SpO_2$  of the patient to the value of the target  $SpO_2$ .

### Pulse oximeter

A conventional pulse oximeter (model 50190, Siemens Medical Electronics, Danvers, MA.) is used to measure  $SpO_2$ . The value from the monitor updates every 3 sec and, according to the manufacturer, utilizes an averaging

algorithm that results in a 6 sec response to a step change of 15% either up or down.

### *Ventilator*

A volume-controlled ventilator (Model 900C, Siemens-Elma AB, Solna, Sweden) is used in the system. The ventilator is equipped with an oxygen fuel cell that measures  $F_{I_{O_2}}$  and a screen pneumotachometer that measures tidal volume ( $V_T$ ) and minute ventilation ( $\dot{V}_E$ ). As the pneumotachometer is located in the ventilator distal to the expired gas tubing, the *measured*  $V_T$  and  $\dot{V}_E$  includes compression volumes. Values from these measurements are provided as calibrated analog signals at the recorder output connector. A second measured  $F_{I_{O_2}}$  from a polarographic  $O_2$  meter (model 04026-03, North American Dräger, Teleford, PA) located in the inspired limb of the breathing circuit is used for verification of the measured  $F_{I_{O_2}}$  from the ventilator.

### *Computer*

The  $Sp_{O_2}$  values from the pulse oximeter, measured  $F_{I_{O_2}}$  and  $\dot{V}_E$  from the ventilator, the verification  $F_{I_{O_2}}$ , and a target  $Sp_{O_2}$  from the user keyboard are input into to a standard personal computer. The output values from the pulse oximeter are acquired via a serial interface. Analog values from the ventilator and the  $O_2$  meter are converted to digital format and input to the computer via a 12 bit A/D multifunction I/O board (model DT-2801, Data Translation, Marlboro, MA). An output control signal to adjust the  $F_{I_{O_2}}$  control mechanism is transmitted from the computer via a digital port of the multifunction board.

Software for I/O, user interface, and all algorithms were written in Microsoft C.

### *$F_{I_{O_2}}$ control mechanism*

The  $F_{I_{O_2}}$  control mechanism consists of a digital circuit, a motor controller, a stepper motor, and a direct mechanical linkage to the control knob of the gas blender of the ventilator. The digital circuit temporarily stores a value from the computer that represents the desired gas blender control knob position. The circuit sets a direction flag, generates the appropriate number of rotation pulses to energize the stepper motor, receives "end of travel" signals from the motor mechanism and disables the motor when appropriate. The geared stepper motor (model TS, Hurst, Princeton, IN) is specified to com-

plete 600 steps per revolution. The  $F_{I_{O_2}}$  control knob of the gas blender rotates  $270^\circ$  over the range of 21% to 100%  $O_2$ . Thus, the nominal resolution of the  $F_{I_{O_2}}$  control mechanism is  $\pm 0.08\% O_2$ .

### *Artifact rejection algorithm*

Recognizing that measurement of  $Sp_{O_2}$  in the clinical setting results in episodes of erroneous or missing data, an artifact rejection algorithm was developed. The logic of this algorithm is based on the notion that when measurements of  $Sp_{O_2}$  are missing or erroneous, the  $Sa_{O_2}$  could actually be falling, rising, or unchanging. Since hypoxemia is a more acute problem than oxygen toxicity, the risk that the  $Sa_{O_2}$  is falling is clearly greatest. Thus, in the absence of reliable data the controller should assume that the  $Sa_{O_2}$  is falling and respond aggressively by increasing the  $F_{I_{O_2}}$ . On the other hand, increasing the  $F_{I_{O_2}}$  when the  $Sa_{O_2}$  was rising or unchanging would produce system instability and a clinically undesirable steady state error. Hence, the risk that  $Sa_{O_2}$  is actually falling should be tempered by the low likelihood that a substantial fall will occur within a few seconds. Thus, we based the algorithm on the assumption that the probability that the  $Sa_{O_2}$  is actually falling increases in proportion to the frequency of artifactual  $Sp_{O_2}$  readings.

We deem a measurement of  $Sp_{O_2}$  as artifactual if its value is more than two standard deviations from a running mean of the previous ten measurements of  $Sp_{O_2}$ . The algorithm replaces an artifactual reading with a pseudo value, which is less than the mean by an amount proportional to the recent frequency of artifactual  $Sp_{O_2}$  values. The pseudo value is then passed on to the controller.

### *Control algorithm*

The clinical control goals for the  $F_{I_x}$  system are distinctly asymmetrical and nonlinear. The permissible undershoot is less than the overshoot, since the risk of hypoxemia is greater than that of excess oxygen exposure for a short period of time. Similarly, the rate of rise of the  $Sp_{O_2}$  should be substantially greater when the measured  $Sp_{O_2}$  is at hypoxemic levels than when it is just below the target. Also, since the  $Sp_{O_2}$  is inherently limited to 100% and is typically near the limit ( $>90\%$ ), the controller output will tend to be biased higher than necessary to achieve zero steady state error.

The system response characteristics are primarily a function of the volumes and flows of the ventilator, breathing apparatus, and patient. As such, it is assumed

that adaptation of the controller for changes in measured  $\dot{V}_E$  are necessary to produce acceptable system response.

To meet these clinical objectives, a classical sampled-data proportional-integral-derivative (PID) controller is used for the main  $SpO_2$  control loop [6]. The algorithm uses gain-scheduling to adjust the proportional gain term relative to the sign and magnitude of the error signal and the minute ventilation ( $\dot{V}_E$ ) [7].

The  $FiO_2$  control loop (minor control loop) uses a sampled-data proportional-integral (PI) controller. The controller is set to make the minor control loop at least an order of magnitude faster than the main  $SpO_2$  control loop to minimize their interaction.

### *Safety subsystem algorithms*

A series of safety features are implemented in hardware and software to prevent inspired mixtures with undesirable low  $FiO_2$  and inadvertent errors in the operation of the system. These include:

1. Alarm threshold values of  $SpO_2$  and  $FiO_2$  are entered into the system by the user. Excursions beyond these limits are visually and audibly annunciated.
2. When communication from the pulse oximeter, or ventilator, or the  $FiO_2$  control mechanism is interrupted, the system: alarms, attempts to set  $FiO_2$  to 100%, and relinquishes mechanical control of the blender to the user.
3. The system monitors the error between the desired  $FiO_2$  (position of the blender control knob) and the measured  $FiO_2$  and alarms if the difference becomes greater than 3% for a period of 30 seconds.
4. A second  $O_2$  meter is used to provide a verification  $FiO_2$  signal. If the two measurements of  $FiO_2$  disagree by more than 5% for a period of 30 seconds, the system alarms and the  $FiO_2$  is forced to 100%.
5. At any time the user may take control of the  $FiO_2$  directly via the computer keyboard or by turning the blender knob manually, thereby disengaging the feedback control system.
6. All measured and computed data values are stored on magnetic media for retrospective analysis.

---

### **SYSTEM TUNING**

---

In order to find control algorithm that would respond to changes in  $Fi_x$  over a wide range of measured  $\dot{V}_E$  and between various subjects in a variety of clinical states, a series of experiments to tune the control algorithm were conducted.

### *Surgical preparation*

All experiments conformed to the standards of the Animal Care Committee, Harvard Medical School. Six adult mongrel dogs weighing 16–23 kg were anesthetized intravenously with sodium pentobarbital ( $40.0 \text{ mg}\cdot\text{kg}^{-1}$ ). After tracheal intubation, the lungs were mechanically ventilated with  $O_2$  in air ( $FiO_2 = 40\%$ ) to maintain normocarbica. Anesthesia was continued throughout the duration of the experiment with sodium pentobarbital ( $1.0 \text{ mg}\cdot\text{kg}^{-1} \text{ q } 45 \text{ min}$ ). Pancuronium bromide ( $0.1 \text{ mg}\cdot\text{kg}^{-1} \text{ prn}$ ) was administered for muscle relaxation.

An arterial cannula was surgically placed in the left femoral artery for blood sampling and to monitor the arterial pressure. A balloon flotation catheter was inserted in a femoral vein, advanced into the pulmonary artery, and connected to an electronic pressure transducer (P231D, Gould-Statham, Oxnard, CA) with a fluid filled, stiff-walled tube. An adult finger probe from the pulse oximeter was placed on the tongue. All hemodynamic variables were recorded on a Grass paper chart recorder.  $FiO_2$ ,  $SpO_2$ ,  $\dot{V}_E$ , RR, and VT were recorded electronically every ten seconds by the  $Fi_x$  system and stored on magnetic diskette.

To simulate respiratory distress syndrome, oleic acid (Aldrich Chemical, Milwaukee, WI) was administered ( $0.1 \text{ mg}\cdot\text{kg}^{-1}$ ) directly into the pulmonary artery.

### *Plant characterization*

To model the response characteristics of the blender, ventilator, breathing apparatus, and the animal's respiratory system, the responses of  $SpO_2$  to periodic step changes in  $FiO_2$  were recorded. Before and following administration of the oleic acid, a sequence of step changes in  $FiO_2$  was made followed by 20 min of measurement of  $SpO_2$ . The  $FiO_2$  was increased from a starting point of 21% in 10% steps until the  $SpO_2$  remained essentially 100%. The  $FiO_2$  was then decreased in 10% steps back down to 21%. Arterial and mixed venous blood was sampled and analyzed (model 170 blood gas system, Ciba-Corning, Medfield, MA) before each change in  $FiO_2$ . In some experiments, the sequence was repeated during hyperventilation and during hypoventilation.

### *Feedback controller*

Based on the appearance of the  $SpO_2$  response to step changes in  $FiO_2$  in the first experiment, the plant model

Table 1. System parameters (mean  $\pm$  1SD) estimated from all step response experiments in six dogs. Time constant ( $\tau$ ) and time delay ( $L$ ) are shown. Parameters were determined at high and low measured  $\dot{V}E$  before and after oleic induced pulmonary distress

	Pre-Pulmonary Injury		Post-Pulmonary Injury	
	Low $\dot{V}E$	High $\dot{V}E$	Low $\dot{V}E$	High $\dot{V}E$
$\tau \pm$ SD	$55 \pm 3$	$49 \pm 3$	$63 \pm 6$	$62 \pm 6$
$L \pm$ SD	$16 \pm 2$	$15 \pm 5$	$23 \pm 2$	$24 \pm 7$

was assumed to consist of a transport delay plus one or two exponential terms. Thus, response data were plotted versus time, a tangent was drawn at the inflection point of each curve, and the time constant of the dominant exponential term was estimated from the slope of the line [8]. The transport delays were estimated directly from the intersection of the tangent with the ordinate axes. Three representative examples of the  $SpO_2$  response of step changes in  $F_{IO_2}$  including the calculated time delay and system time constants are shown in Figure 2. Table 1 lists the calculated system parameters for all of the animals prior to and following administration of oleic acid.

After each experiment, feedback controller coefficients were revised to produce acceptable system response for all subjects (e.g. zero steady-state error and undershoot or overshoot less than 20% of the change). Also, gain-scheduled control functions were tuned to make the controller more aggressive when the  $SpO_2$  error signal was greater than approximately 3% and to account for the effect of  $\dot{V}E$  on the model transport delays and time constants of the plant. A plot of the proportional gain coefficient (Figure 3 upper panel) shows that the feedback controller is scheduled to the value of  $SpO_2$  error signal. Similarly, Figure 3 (lower panel) shows that the gain coefficients are further scheduled to  $\dot{V}E$ . The lower panel of Figure 4 is an example of the system response to a lowering of the target  $SpO_2$ . The response is considerably less aggressive than the upper panel of Figure 4 where the target  $SpO_2$  was reset at a higher value than the current  $SpO_2$ .

At the end of the experiment, the most recent version of the feedback controller software was tested by closing the feedback loop and setting a target  $SpO_2$  in the range 90%–97%. An example of the response of the final system design with the feedback loop closed is shown in Figure 5. Note the slight overshoot and steady state error within  $\pm 2.5\%$  of the  $SpO_2$  signal.

## Artifact rejection

Segments of data collected during the animal experiment that were visually judged to be artifact free were modified to test the artifact rejection algorithm. Various data points from the segments were replaced with aberrant values to simulate missing or artifactual  $SpO_2$  readings. These data strings were then input to the  $F_{I_x}$  feedback system in place of real pulse oximeter readings. The resulting behavior of the control system was evaluated.

The artifact rejection algorithm is demonstrated in Figure 6, where the response of the system is compared with the rejection algorithm active (upper panel) and inactive (lower panel). In these simulations,  $SpO_2$  values of zero have been substituted periodically. When the algorithm is active, pseudo values of  $SpO_2$  are substituted resulting in a small increase in  $F_{IO_2}$  during and following the artifacts. The measured  $SpO_2$  remains near the target. However, with the artifact rejection algorithm inactive, the  $F_{IO_2}$  increases dramatically during and following each episode. The measured  $SpO_2$  is chronically higher than the target.

## Safety subsystems

The safety subsystems were tested by simulating mishaps in the system and observing the appropriate response. Excursions of the measured values beyond the alarm thresholds were simulated by replacing the pulse oximeter signal with a communication link to a second computer. Loss of the communication from pulse oximeter, ventilator, and  $F_{IO_2}$  control mechanism were simulated by disconnecting each of the sensors. Erroneous blender behavior was simulated by loosening the mechanical coupling from the motor and turning the blender knob by hand. Disagreement between the  $F_{IO_2}$  meters was simulated by manually changing the offset or gain control of one of the meters. All safety subsystems performed as designed.

## DISCUSSION

A system to automatically maintain  $SpO_2$  to a user selected value by adjusting the  $F_{IO_2}$  of a mechanical ventilator using negative feedback control has been developed. Parameters for feedback control have been determined and an artifact rejection algorithm, and various safety features have been designed, built, and tested.

The response of animals to change in  $F_{IO_2}$  appears to be a monotonic change in  $SpO_2$  generally characterized

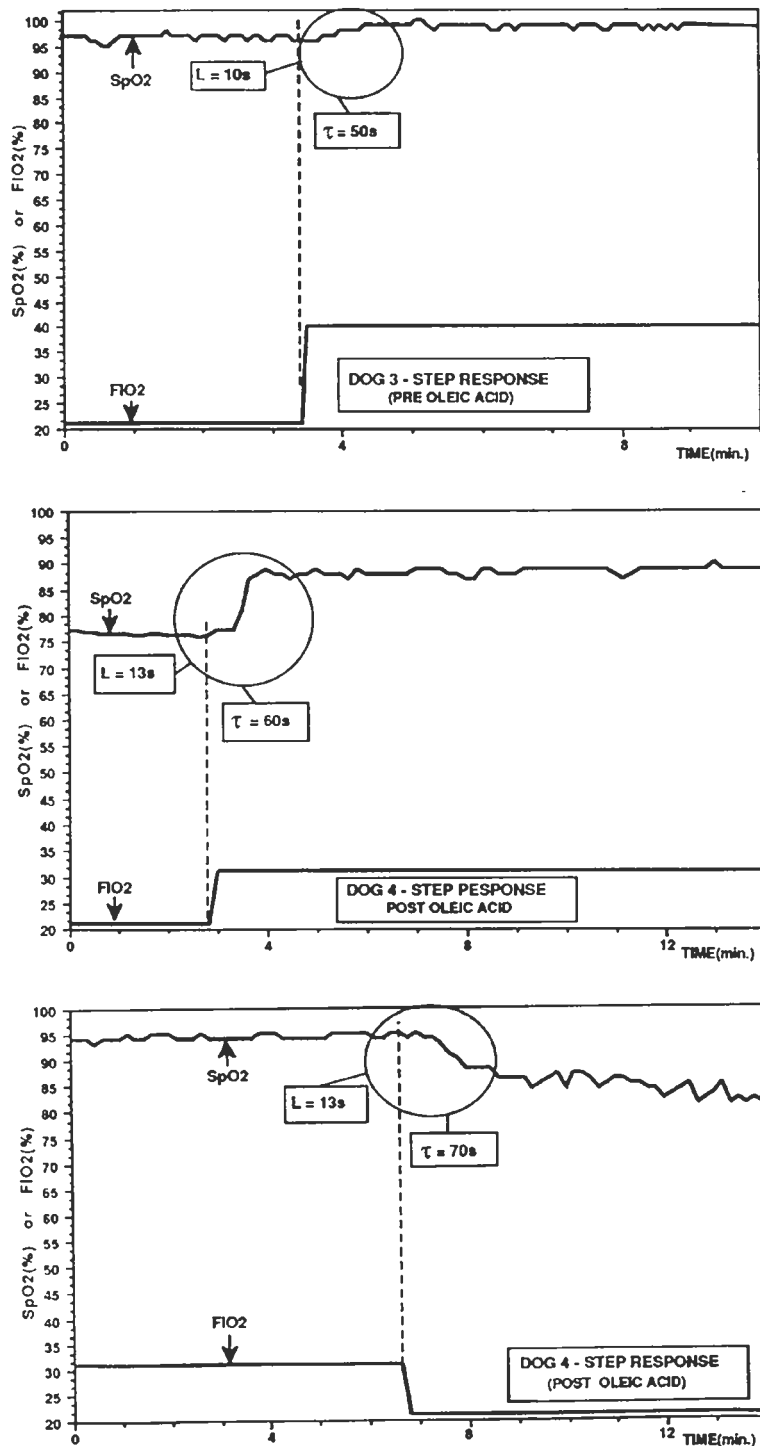


Fig. 2. Representative examples of the response of SpO<sub>2</sub> to step changes in FIO<sub>2</sub>. The upper panel shows the SpO<sub>2</sub> response of a dog with a healthy pulmonary system to a step change in FIO<sub>2</sub> from room air to 40% O<sub>2</sub>. A calculated time delay (L) of 10 s and time constant ( $\tau$ ) of 50 seconds are shown. The middle panel shows the response of SpO<sub>2</sub> of a dog with a oleic acid induced pulmonary distress to a step change in FIO<sub>2</sub> from room air to 30% O<sub>2</sub>. A calculated time delay (L) of 13 s and  $\tau$  of 60 seconds are shown for the substantial increase in SpO<sub>2</sub> from about 78% to about 90%. The lower panel shows the SpO<sub>2</sub> response of a dog with oleic acid induced pulmonary distress to a downward step change in FIO<sub>2</sub> from 30% to room air. A calculated time delay (L) of 13 s and  $\tau$  of 70 seconds are shown for the substantial decrease in SpO<sub>2</sub> from about 95% to about 85%.

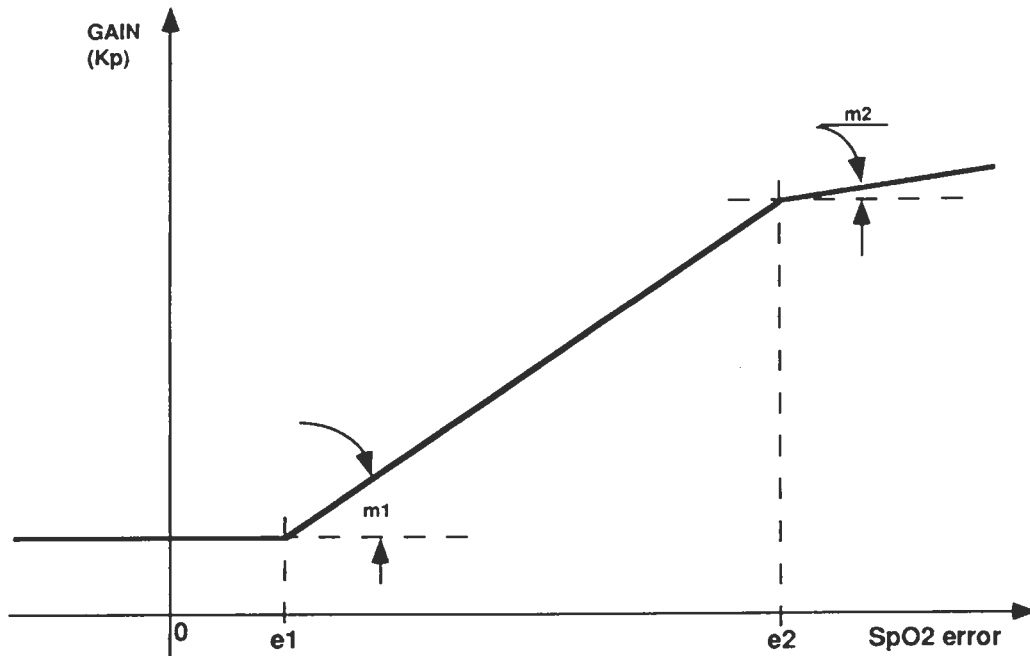


Fig. 3. upper panel. A plot of the offset of the proportional gain feedback coefficient ( $K_{p_o}$ ) as a function of measured  $\dot{V}_E$ . The offset is continuously variable between break points  $\dot{V}_{E_0}$  and  $\dot{V}_{E_1}$ , at a slope,  $-K_{mv}$ . Values of  $\dot{V}_{E_0}$  and  $\dot{V}_{E_1}$  are approximately 1.2 and 5.5 L, respectively.

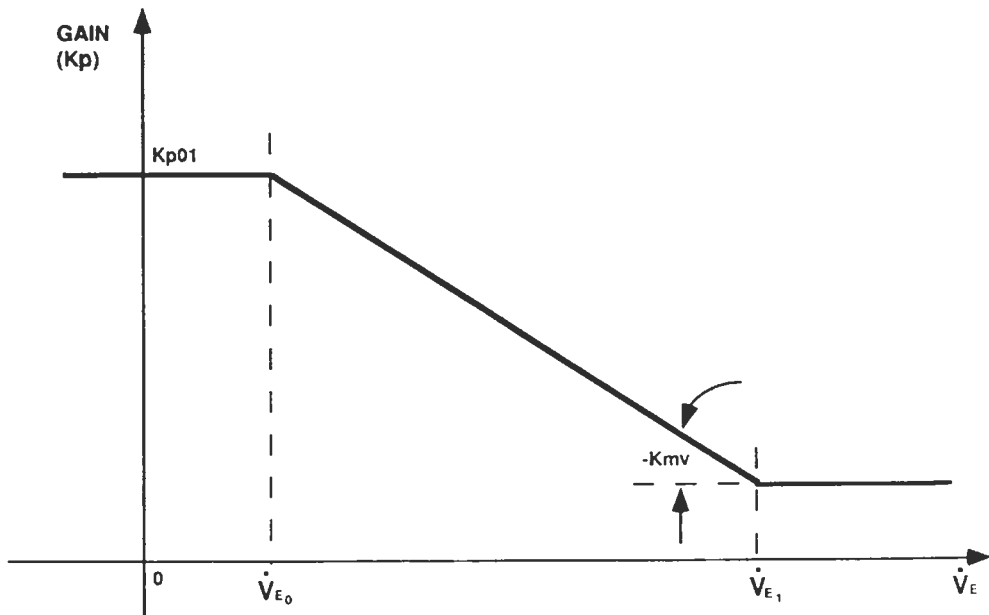


Fig. 3. lower panel. A schematic plot of the proportional gain feedback coefficient ( $K_p$ ) showing the gain as a function of the  $SpO_2$  error. Particular break points,  $e_1$  and  $e_2$ , and slopes of the relationship,  $m_1$  and  $m_2$ , are depicted. Values for  $e_1$  and  $e_2$  are 3% and 12%, respectively. Note that the offset  $K_{p_o}$  is a function of measured  $\dot{V}_E$  as shown in the lower panel.

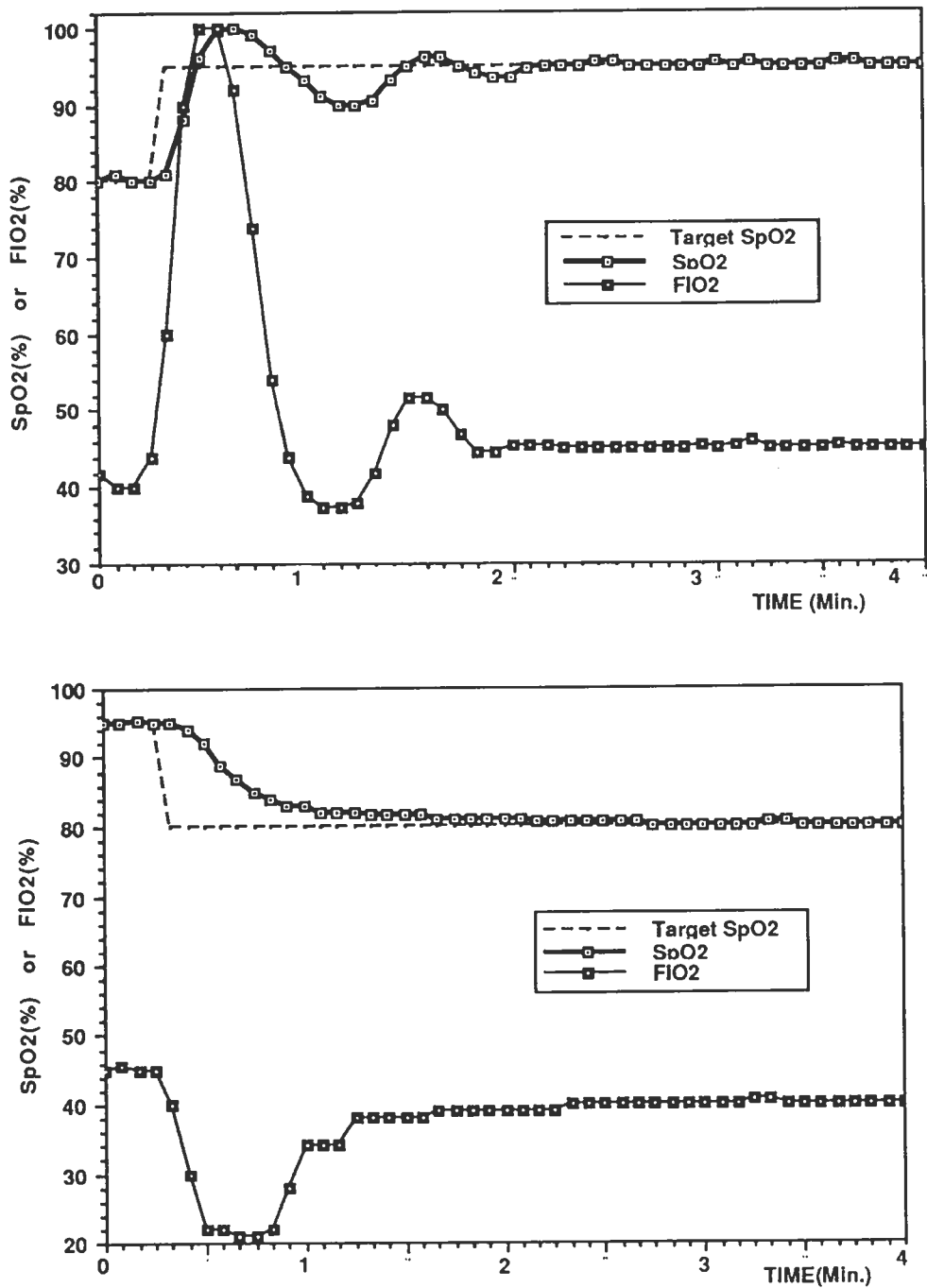


Fig. 4. Examples of the system response to a change of the target SpO<sub>2</sub> during simulation experiments. The upper panel shows a change in target SpO<sub>2</sub> from 80% to 95%. The lower panel shows a change in target SpO<sub>2</sub> from 95% to 80%. The system response shown in the lower panel is considerably less aggressive than the upper panel where the target SpO<sub>2</sub> was reset at a higher value than the current SpO<sub>2</sub>.

by a time delay and one or two time constants. The amplitude of the response is not strictly linear, as demonstrated by relatively smaller changes in SpO<sub>2</sub> for a given change in FiO<sub>2</sub> when the SpO<sub>2</sub> approaches 100%. This

is due to the nonlinear shape of the oxyhemoglobin dissociation curve. Although, the non-linearity does not affect the steady state error of the feedback control system, the transient response can be problematic. Gen-



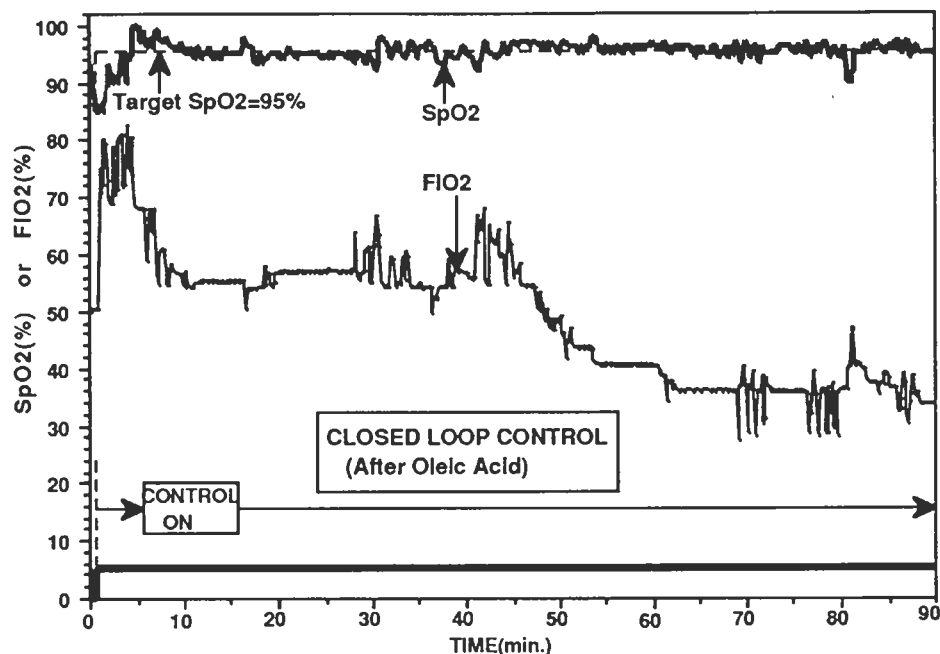


Fig. 5. An example of the response of the  $F_{I_x}$  system with the feedback loop closed. A target  $SpO_2$  of 95% over a 90 minute epoch is shown for a dog with oleic acid induced pulmonary distress. Note the decreasing  $O_2$  requirement while the  $SpO_2$  is maintained at the target by the system.

erally, we have used nonlinear gain scheduling to eliminate unstable or under-damped response.

Both the time delay and at least the first time constant appear to be lengthened by oleic acid induced respiratory distress. This phenomenon is probably attributable to loss of functional alveolar surface area (resulting in increased ventilation-perfusion mismatch and shunt), prolonged diffusion of  $O_2$  across alveolar capillary membrane, and an increase in dead space. A circulatory response to the respiratory insult could also result in a prolonged circulation time to the peripheral  $SpO_2$  measurement site. Regardless of the mechanism, the controller must be dampened to accommodate the slower response during respiratory distress.

The range of the plant response parameters seen among the animals tested suggests that an auto-tuning control method where periodic measurements of response using small signals or pseudo-random noise are used to adjust the controller may be indicated.

The adaptive algorithm (gain scheduling) that compensates for  $\dot{V}_E$  has been developed using only a limited range of measured  $\dot{V}_E$  values. Although this adaptation appears to improve the system response by keeping the overshoot and undershoot well below 20%, a broader range of measured  $\dot{V}_E$  values needs to be examined.

The safety mechanisms for the system anticipate many of the potential system failures that could lead to an unsafe condition for a patient. Less obvious failure modes

may exist and will have to be uncovered with further testing of the controller.

The plant response parameters seen in the animal experiments would be expected to be somewhat different than those in humans. Thus, further development would require changing the control systems accordingly. For example, the circulation time from a human finger is known to be substantially longer than that from a dog's tongue making the measurement lag for  $SpO_2$  greater. System instability might result if the feedback controller was not modified appropriately.

The  $F_{I_x}$  controller system successfully functions to achieve and maintain a target  $SpO_2$ . The question remains how such a system compares with conventional ICU management techniques with respect to minimizing the exposure to high concentrations of  $O_2$  for prolonged periods of time while preventing periods of hypoxemia in mechanically ventilated patients with severe respiratory impairment.

---

The laboratory assistance of Tom Manning and Ignatius Calalang is greatly appreciated. The authors gratefully acknowledge the encouragement and assistance of Fred Geheb, PhD, and Susan Dress. This work was supported in part by a grant from Siemens Medical Electronics, Danvers, MA.

---

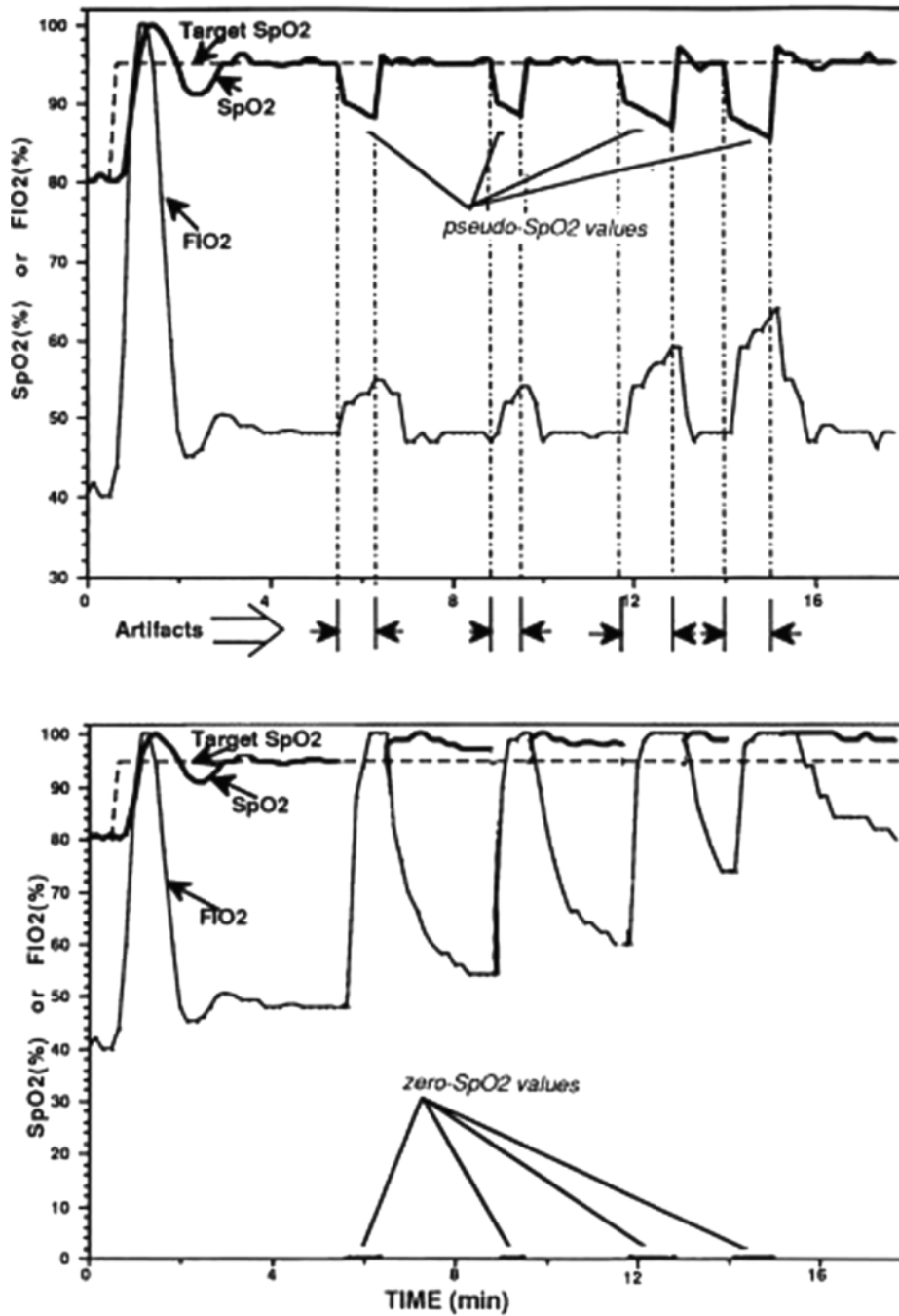


Fig. 6. Examples of the artifact rejection algorithm performance with the rejection algorithm active (upper panel) and inactive (lower panel). In these simulations, SpO<sub>2</sub> values of zero have been substituted periodically. When the algorithm is active, pseudo values of SpO<sub>2</sub> are substituted resulting in a small increase in FIO<sub>2</sub> during and following the artifacts. The measured SpO<sub>2</sub> remains near the target. However, in the lower panel with the artifact rejection algorithm inactive, the FIO<sub>2</sub> increases dramatically during and following each artifact episode. The measured SpO<sub>2</sub> is chronically higher than the target.

---

**REFERENCES**

---

1. Nunn JF. Applied Respiratory Physiology (3rd Edition) Boston: Butterworths, 1987: 493–494.
2. Kafer ER. Pulmonary oxygen toxicity: A review of the evidence for acute and chronic oxygen toxicity in man. *Brit J Anaesth* 1971; 43: 687–692.
3. Yu C, He WG, So JM, Roy R, Kaufman H and Newell JC. Improvement in arterial oxygen control using multiple-model adaptive control procedures. *IEEE Trans Biomed Engr* 1987; 34: 567–574.
4. Tehrani FT. A microcomputer oxygen control system for ventilatory therapy. *Annals of Biomed Engr* 1992; 20: 547–558.
5. Kaysuya H and Sakanashi Y. Simple and noninvasive indicator of pulmonary gas exchange impairment using pulse oximetry. *J Clin Monit* 1989; 5: 82–86.
6. Kuo BC. Digital Control Systems. New York: Holt, Rinehart and Winston, 1980: 509–514.
7. Astrom KJ and Wittenmark B. Adaptive Control. Reading MA: Addison-Wesley, 1989: 343–370.
8. Franklin GF. Feedback Control of Dynamic Systems. Reading, MA: Addison-Wesley, 1986: 104.